August 1976 KFK 2342

Institut für Angewandte Kernphysik

Excitation Functions of $^{191+193}Ir$, ^{197}Au (^{6}Li,xn + yp) Compound Nuclear Reactions at $E_{Li} = 48 - 156$ MeV

J. Kropp, H. Klewe-Nebenius, J. Buschmann, H. Rebel
H. Faust, H. J. Gils, J. Rieder, K. Wisshak

GESELLSCHAFT
FÜR
KERNFORSCHUNG M.B.H.

KARLSRUHE

Als Manuskript vervielfältigt

Für diesen Bericht behalten wir uns alle Rechte vor

GESELLSCHAFT FÜR KERNFORSCHUNG M. B. H.

KARLSRUHE

KERNFORSCHUNGSZENTRUM KARLSRUHE

KFK 2342

Institut für Angewandte Kernphysik

Excitation Functions of $^{191+193}Ir$, $^{197}Au(^{6}Li,xn+yp)$ Compound Nuclear Reactions at E_{Li}=48-156 MeV

J. Kropp[+], H. Klewe-Nebenius[+], J. Buschmann, H. Rebel
H. Faust[+], H.J. Gils, J. Rieder[+] and K. Wisshak

[+]Physikalisches Institut der Universität Heidelberg

Gesellschaft für Kernforschung mbH, Karlsruhe

ABSTRACT

Excitation functions of the compound nuclear reactions $^{191+193}Ir$, ^{197}Au (^{6}Li,xn+yp) for x=3-13 and y=1,2 have been investigated by means of 'in beam' γ-ray spectroscopy at the 156 MeV ^{6}Li beam of the Karlsruhe Isochronous Cyclotron. The beam energy has been varied in the range of 48 to 156 MeV in steps of about 10 MeV by Be-absorber foils in the external beam line. Absolute cross sections have been determined by normalizing the measured γ-ray intensities to the production cross sections of K-X-rays in the target. The experimental excitation functions are discussed on the basis of predictions of the preequilibrium (hybrid) model. While in most cases the theoretical calculations fairly well reproduce energy position and shapes of the curves, strong discrepancies in the absolute scale of the cross sections are observed. The theoretical predictions overestimate the (^{6}Li,xn) cross sections by a factor of about 6. Conspicuous anomalies have been detected when comparing the (^{6}Li,xn+1(2)p) reactions with (^{6}Li,xn) reactions. The reactions with emission of one or two protons are considerably enhanced. The discrepancies and anomalies observed are tentatively explained by the influence of the ^{6}Li break-up, which experimentally proves to be the dominant contribution to the total reaction cross section. The enhancement of the reactions with emission of protons may be a consequence of a cluster effect in preequilibrium emission process (cluster transfer into highly excited states).

Anregungsfunktionen von $^{191+193}Ir$, $^{197}Au(^{6}Li,xn+yp)$-Compoundkern-Reaktionen bei E_{Li} = 48 - 156 MeV

Zusammenfassung:

Am 156 MeV ^{6}Li-Strahl des Karlsruher Isochron-Zyklotrons wurden Anregungsfunktionen der Compoundkern-Reaktionen $^{191+193}Ir$, $^{197}Au(^{6}Li,xn+yp)$ mit x = 3 bis 13 und y = 1,2 untersucht. Die primäre Strahlenergie wurde mit Be-Absorbern in Schritten von ca. 10 MeV zwischen 156 und 48 MeV variiert. Aus "in-beam" γ-Spektren wurden absolute Wirkungsquerschnitte durch Normierung auf die von den Projektilen im Target erzeugte K-Röntgenstrahlung bestimmt. Die gemessenen Anregungsfunktionen wurden mit Vorhersagen des Hybridmodells von Blann verglichen. Es zeigte sich, daß Lage und Form der Kurven in den meisten Fällen gut reproduziert werden, während die absoluten Wirkungsquerschnitte erhebliche Abweichungen aufweisen. Im Fall der $(^{6}Li,xn)$-Reaktionen überschätzt die Theorie die Wirkungsquerschnitte um einen Faktor 6. Im Vergleich hierzu zeigen Reaktionen mit 1 oder 2 Protonen im Ausgangskanal deutlich größere Wirkungsquerschnitte. Diese Diskrepanzen können möglicherweise durch den starken ^{6}Li-Aufbruchkanal erklärt werden, wobei der erhöhte Wirkungsquerschnitt der $(^{6}Li,xn+yp)$-Reaktionen als Folge einer Clusterbildung interpretiert werden könnte, bei dem eines der Clusterteilchen (α oder d) in einen hochangeregten Zustand des Targetkerns eingefangen wird und Compoundkern-Reaktionen vom Typ $(\alpha,xn+yp)$ bzw. $(d,xn+yp)$ auslöst, während das andere Teilchen in einem direkten Prozess reemittiert wird.

1. Introduction

Investigations of compound nuclear reactions have several purposes. In addition to the practical aspects looking for optimum conditions of producing nuclei far off the line of stability the excitation functions provide interesting information on the reaction mechanism and on the relaxation processes of highly excited nuclei. With this view excitation functions for reactions induced by various light projectiles (p,d,α) have been measured up to energies of the incident particles of about 50 MeV/nucleon, while measurements with heavier projectiles (A > 4) are very scarce in the high energy region. An extension to higher energies, however, is of particular interest as there are experimentally observed deviations from early statistical descriptions of the processes (Weisskopf-Ewing model [1]) by preequilibrium emission of high energetic nucleons. The preequilibrium decay of highly excited nuclei is assumed for explaining the distinct high energetic tails of the observed excitation functions and is included into various theoretical model descriptions [2)-9)].

In the present paper we report on measurements of excitation functions of (^{6}Li,xn+yp) reactions up to projectile energies E_{Li} = 156 MeV. The measurements were done at the ^{6}Li beam [10] recently installed at the Karlsruhe Isochronous Cyclotron. The results not only inform on the nuclidic regions accessible by using high energy ^{6}Li ions but also provide an experimental test of some assumptions and procedures of current theoretical models describing the reaction mechanism. Though in general the experimental observations with deuterons and α-particles find a satisfactory agreement with theoretical predictions of the preequilibrium model [11),12)], there are also indications that the absolute values of the cross sections are systematically overestimated by the models. Considering ^{6}Li projectiles some particular features may be expected due to the presence of a strong direct reaction channel by Li break-up. As in the currently used procedures calculating the compound nucleus formation the contribution of direct channels to the total cross section is taken into account only very globally [13)] the break-up (and other competing reaction channels as e.g. nuclear fission) may reveal systematic discrepancies and require some refinements of the model descriptions.

Zum Druck eingereicht am 23.8.1976

2. Experimental Procedures

2.1 Experimental Setup

The (^{6}Li,xn+yp) reactions have been identified via the prompt γ-rays emitted by the produced final nuclei. The γ-spectroscopic measurements have been performed at the external beam line of the Karlsruhe Isochronous Cyclotron. Special precautions were necessary in order to reduce the strong background due to the large number of evaporated neutrons and high energy secondary particles (e.g. from ^{6}Li break-up). A small, thin-walled and properly shielded target chamber was installed as far away as possible from massive components of the beam line system. It has been found that even scattering from the residual gas in the beam line influences the background conditions if the beam line pressure is not less than 10^{-3} - 10^{-4} Torr [+]. By the final arrangement a background reduction of a factor 5 has been achieved compared to the set up used in our previous γ-spectroscopic experiments at the 104 MeV α-particle beam [14]. The γ- and X-ray spectra have been measured by alternative one of two Ge(Li)-detectors both with an energy resolution of 2.1 keV FWHM and with a relative efficiency of ca. 15 % for the 1332 keV γ-rays of ^{60}Co. Absolute efficiency curves (fig. 1) were determined using ^{57}Co, ^{166m}Ho, ^{182}Ta, ^{198}Au sources and an intensity calibrated ^{60}Co source in an arrangement identical to the setup at the beam line thus including absorption of target chamber windows. The error bars indicated in fig. 1 include statistical errors and uncertainties of the relative intensity values which have been taken from literature.

The irradiated targets were metallic foils of 25 mg/cm^2 Au and of 112 mg/cm^2 natural Ir. The choice of these targets had the following aspects:

(i) In both targets (^{6}Li,xn+yp) reactions produce Hg isotopes the main γ-transitions of which are well known and appropriate for identification up to isotopes with large neutron deficit.

(ii) A cross bombardment of Au and Ir can support the identification of individual γ-rays in several cases.

(iii) Homogeneous Au targets can be easily prepared thin enough that absorption of low energy γ- and X-rays in the targets remains negligible, but also thick enough to obtain sufficient γ-intensity even for very small beam currents.

[+] Some effects of a bad vacuum and the origin of its influence on the background are discussed in ref. 17.

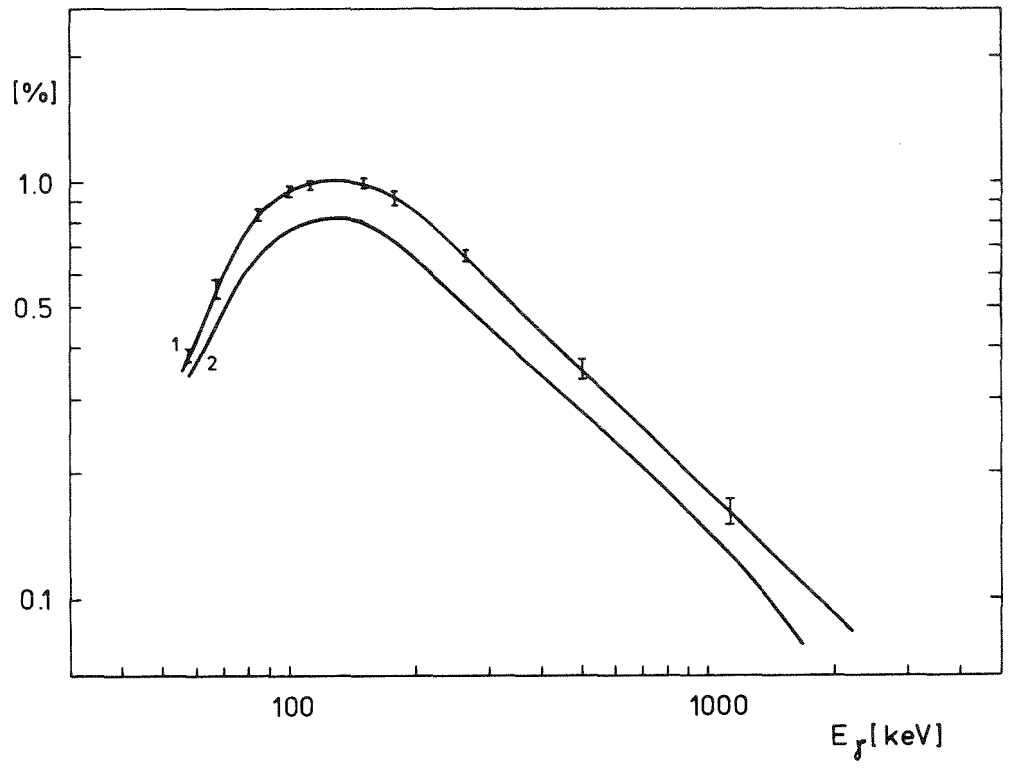

Fig. 1: Photo peak efficiencies of the two Ge(Li) detectors in the experimental setup used.

In the case of Ir, however, we did not succeed to get sufficiently thin foils so that corrections due to self absorption, in particular of the X-rays and due to the energy loss of the ^{6}Li ions, were necessary.

2.2 Energy Variation of the ^{6}Li Beam

The primary ^{6}Li beam energy of 156 MeV has been degraded by Be-absorber foils [25] in steps of about 10 MeV down to E_{Li} = 48 MeV; in some cases intermediate energy values have been chosen additionally. From tables the energy losses in Be are known for ^{7}Li ions up to an energy of 80 MeV so that an extrapolation for ^{6}Li ions of higher energies was necessary. In order to check the calculated values of the residual ^{6}Li energies experimentally, we compared the magnetization currents of the switching magnet of the external beam line for ^{6}Li- and α-particles, respectively, at different beam energies. For the energy degraded α-particle beam the residual energies are sufficiently well known. Taking the residual energies the magnetization current can be calibrated in terms of the relativistic velocities of the particles for both cases. The fair agreement of the both curves shown in fig. 2 gives some confidence in the calculated values of the ^{6}Li residual energies. The deviations correspond to an overall energy uncertainty of the incident ^{6}Li ions of about 2 MeV.

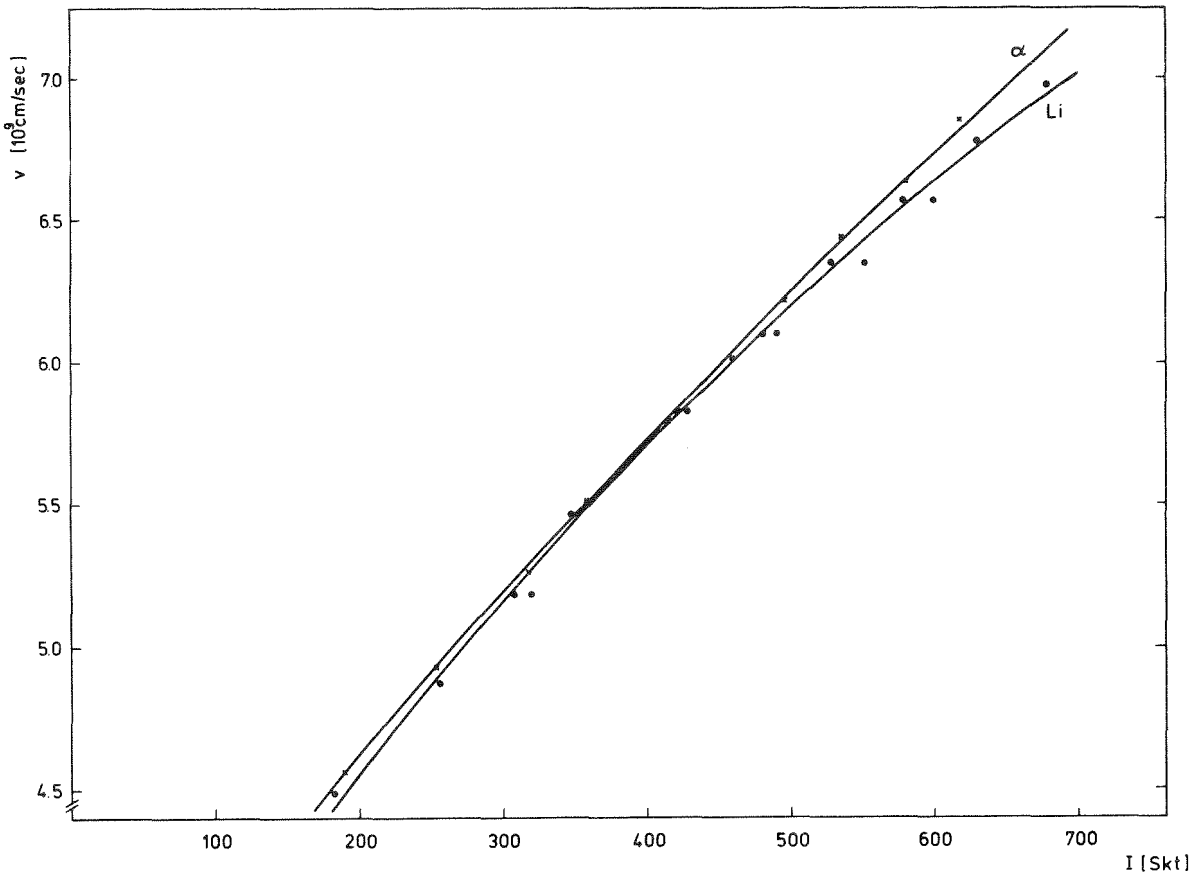

Fig. 2: Relativistic velocities calculated from the residual energies of the energy degraded α-particle and ^{6}Li beams as functions of the magnetization current (arbitrary units) of the switching magnet.

Additional uncertainties in the energy scale of the excitation functions arise from energy losses of the ^{6}Li-ions in the targets: the energy losses vary in the energy range of E_{Li} = 156 - 48 MeV between 2 and 4.7 MeV for the Au target and between 9 and 21 MeV for the Ir target. Because of these relatively large energy losses in the target, the compound nuclear reactions in the threshold region can occur only in a thin layer of the upstream surface of the target. In general, we determine the cross sections averaged over the energy range ΔE_o of the losses in the target at the incident energy E_o. Provided that theoretical excitation functions $\sigma(E)$ reproduce the energy dependence sufficiently well the effects of the energy losses in the targets can be estimated and converted into an energy shift of the experimental point considered. This energy shift

$$\Delta E = E_o(\sigma_o) - E(\sigma_{corr}) \qquad (2.2.1)$$

is obtained from

$$\sigma_{corr} = \frac{1}{\Delta E_o} \int_{E_o - \Delta E_o}^{E_o} \sigma(E')dE' \qquad (2.2.2)$$

by reading the respective energy value $E(\sigma_{corr})$ from the theoretical excitation function $\sigma(E)$. The uncertainties in the energy scale due to this correction is less than 3 MeV even in extreme cases. The total energy uncertainty varies between 3 and 5 MeV for beam energies from 156 to 48 MeV, respectively.

2.3 Determination of Absolute Cross Sections

For determination of absolute cross sections the measured γ-ray intensities have to be normalized to the number of target nuclei/cm^2 (N_{Targ}) and the number of incident particles (N_{Li}). In the arrangement used the measurement of the beam current and the integrated charge with a Faraday cup seemed to be less applicable because of the difficulties arising from the beam divergence of the energy degraded beam due to the straggling in the Be absorbers and in the thick target. Experimental studies with the α-particle beam had shown that there are intensity losses of up to 30 % for the lower energies (See ref.17). For these reasons we preferred a normalization of the γ-ray yields to the X-ray intensities (I_x) produced by the interaction of the projectiles with the target atoms. The cross section for the K-X-ray production can be written

$$\sigma_x = \frac{I_x}{N_{Li}\, N_{Targ}} \quad \frac{1}{B_x \cdot \Omega \cdot \varepsilon_x} \qquad (2.3.1)$$

with B_x = the X-ray self absorption and ε_x = the absolute X-ray efficiency of the detector. The cross section σ_x is related to the K-shell ionization cross section σ_I by

$$\sigma_x = \omega_K \cdot \sigma_I \qquad (2.3.2)$$

with ω_K = the fluorescence yield of the K-shell of the target element considered and tabulated in ref.[15]. Values of the ionization cross sections σ_I can be taken with some confidence from theoretical calculations of Garcia [16]. The compound nuclear cross section is then given by

$$\sigma(E) = \frac{I_\gamma}{N_{Li}\, N_{Targ}} \quad \frac{1}{\Omega \cdot \varepsilon_\gamma} = \frac{I_\gamma}{\varepsilon_\gamma rel} \cdot F(E) \qquad (2.3.3)$$

Target	ω_K	$B_x \cdot \epsilon_x^{rel}$	E_{Li} [MeV]	I_x [10^6]	σ_I [barn]	F(E) [μbarn]
$^{191+193}$Ir	0.962	0.326	156	6.97	24.34	0.85
			146.6	4.01	21.39	1.30
			137.4	5.53	18.29	0.81
			127.5	5.34	15.50	0.71
			117.4	1.48	12.71	2.1
			106.7	1.63	9.92	1.49
			102.0	1.87	8.84	1.15
			93.2	1.35	6.82	1.23
			83.6	1.88	4.96	0.64
			73.2	2.04	3.41	0.41
			67.3	1.11	2.64	0.58
			61.6	1.55	1.86	0.29
			56.6	0.89	1.55	0.43
			48.4	1.30	0.93	0.17
^{197}Au	0.964	0.62	156	6.11	22.82	1.76
			146.6	1.66	19.60	5.52
			137.4	3.17	16.10	2.34
			127.5	3.42	13.72	1.84
			117.4	2.22	11.62	2.43
			113.5	0.06	11.06	86.2
			106.7	2.00	9.24	2.18
			102.0	1.37	8.26	2.84
			93.2	0.76	6.44	3.93
			83.6	1.28	5.04	1.84
			73.2	1.71	3.64	1.00
			61.6	1.67	2.38	0.67
			48.4	0.79	1.26	0.75

Tab. 1: Measured X-ray intensities and values of various quantities used in eq. 2.3.3.

where the energy dependent factor F(E) is determined by I_x, $\sigma_I(E)$ and the r e l a t i v e efficiency of the detector for X-rays. Details of the procedure applied and the parameters specifying σ_I are discussed elsewhere [17]. The obvious advantages of this method are the following:

(i) the procedure relates directly to the product $N_{Li}\ N_{Targ}$ independently from spot size of the beam and the knowledge of thickness and homogeneity of the target

(ii) only relative efficiencies of the detector for X- and γ-rays have to be known.

On the other hand, the procedure requires the knowledge of the K-ionization cross sections which actually involves an interpolation using a theory [16] and thus implying some uncertainties (~15 %). Additionally, the relative large energy spread of the beam in the target requires an averaged value of σ_I for thick targets and lower energies.

In tab. 1 the values of the measured X-ray intensities and of various quantities used for calculating absolute cross sections from the measured γ-ray yields are compiled.

The procedure has been checked at the maximum ^{6}Li energy where the beam current integration can be assumed to be sufficiently accurate. In tab. 2 we compare the normalization factors F(E) deduced from the current integration and from the X-ray measurements for the Au and Ir target. The differences are within the experimental uncertainties.

Target	$F_{current}$ [μbarn]	$F_{X\text{-}ray}$ [μbarn]
^{197}Au	2.2	1.8
$^{191+193}$Ir	0.77	0.85

Tab. 2: Normalization factors for beam current integration and X-ray normalization at E_{Li} = 156 MeV

An additional contribution to the X-ray intensity originates from K-X-rays accompanying electron capture or internal conversion after (^{6}Li,xn+2p) and (^{6}Li,xn+3p) reactions, since in the considered nuclidic region the values of compound nuclear cross sections and of ionization cross sections are expected to be roughly of the same order of magnitude. An estimate of this contribution can be obtained from the intensity of the X-rays correlated to (^{6}Li,xn) and (^{6}Li,xn+p) reac-

tions shown in the X-ray spectra of fig. 3. From the theoretical relative cross sections of xn+2p, xn+3p reactions an upper limit for the (xn+3p) contribution can be derived even in the case that secondary reactions induced by ^{6}Li break-up particles (c.f. Sec. 3.2) have to be taken into account. For a ^{6}Li energy of 48 MeV this upper limit amounts to be 1 % and becomes even smaller for higher projectile energies.

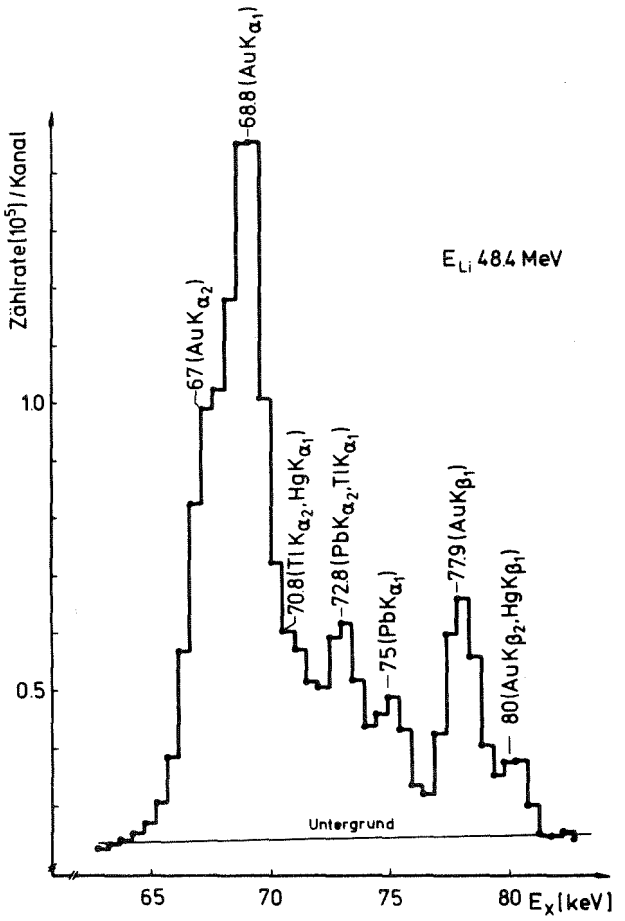

Fig. 3: X-ray spectra induced by ^{6}Li ions in an Au target

2.4 Measurements and Results

In beam γ-ray spectra have been measured during the irradiation of the Au and Ir targets with ^{6}Li ions of 48 - 156 MeV. Neutron deficient isotopes of Pt, Au, Hg, Tl and Pb have been identified from at least 3 known γ-rays (energies and relative intensities). In the case of the Hg isotopes ^{186}Hg could be produced by a $^{191+193}$Ir(^{6}Li, (11+13)n) reaction. This demonstrates the possibility to produce very neutron deficient nuclei by higher energy ^{6}Li ions. Tab. 3 compiles the identified nuclei and γ-rays used for the construction of the excitation functions. Mostly the transitions to the ground state or to an isomeric state which in general represent 100 % production intensity have

Target	Reaction	Final Nucleus	Transition	Energy [keV]	Relat. Intensity
$^{191+193}Ir$	3n+5n	^{194}Hg	$2^+ \rightarrow 0^+$	427.9	1
	4n+6n	^{193}Hg	$21/2^+ \rightarrow 17/2^+$	622.4	(0,9)
	5n+7n	^{192}Hg	$2^+ \rightarrow 0^+$	422.8	1
	6n+8n	^{191}Hg	$19/2^+ \rightarrow 17/2^+$	781	0.21
	7n+9n	^{190}Hg	$2^+ \rightarrow 0^+$	416.2	1
	9n+11n	^{188}Hg	$4^+ \rightarrow 2^+$	591.4	0.63
	10n+12n	^{187}Hg	$21/2^+ \rightarrow 17/2^+$	599	(0.9)
	11n+13n	^{186}Hg	$8^+ \rightarrow 6^+$	424	0.5
	(3n+5n)+p	^{193}Au	$15/2^- \rightarrow 11/2^-$	407.8	1
	(5n+7n)+p	^{191}Au	$15/2^- \rightarrow 11/2^-$	419.9	1
^{197}Au	5n	^{198}Pb	$4^+ \rightarrow 2^+$	562.4	0.95
	7n	^{196}Pb	$2^+ \rightarrow 0^+$	1049.1	1
	9n	^{194}Pb	$2^+ \rightarrow 0^+$	964.2	1
	5n+p	^{197}Tl	$11/2^- \rightarrow 9/2^-$	387.7	1
	7n+p	^{195}Tl	$11/2^- \rightarrow 9/2^-$	394.3	1
	9n+p	^{193}Tl	$11/2^- \rightarrow 9/2^-$	392	1
	11n+p	^{191}Tl	$11/2^- \rightarrow 9/2^-$	387	1
	6n+2p	^{195}Hg	$17/2^+ \rightarrow 13/2^+$	371.2	1
	7n+2p	^{194}Hg	$8^+ \rightarrow 6^+$	564	0.3
			$5^- \rightarrow 4^+$	748	(0.6)
	8n+2p	^{193}Hg	$29/2^+ \rightarrow 25/2^+$	617.7	0.29
			$29/2 \rightarrow 25/2$	302.5	0.29
	9n+2p	^{192}Hg	$2^+ \rightarrow 0^+$	422.8	1
	10n+2p	^{191}Hg	$15/2^+ \rightarrow 13/2^+$	535.3	0.34
	11n+2p	^{190}Hg	$2^+ \rightarrow 0^+$	416.6	1
			$4^+ \rightarrow 2^+$	625.4	0.95

Tab. 3: γ-transitions used for the construction of the (^{6}Li,xn+yp) excitation functions. Relative intensities given in brackets have been determined in the present experiments from other transitions with known intensities of the respective nuclide. The references for the quoted data are compiled in ref. [17].

been used, except of such cases where closely lying γ-rays from neighbouring nuclei disturb a reliable intensity determination. Figs. 4 and 5 display some of the complex γ-spectra which have been evaluated by use of a computer program (with an uncertainty in the intensity values of 5-15 %). Some additional uncertainties arising from several sources are listed in tab. 4.

The error due to the angular distribution is an upper limit when considering transitions with different multipolarity. Together with the statistical error of I_γ a total error of 20-25 % is estimated for the measured cross sections.

As can be seen in figs. 4 and 5 the strongest γ-rays originate from (xn+p) reactions in contrast to theoretical model calculations predicting (xn+yp) reactions with appreciably smaller cross sections than for the corresponding (xn) reactions. This is also indicated by the ratios of the K-X-ray intensities corresponding to (xn), (xn+p) and (xn+2p) reactions where a conspicuous enhancement of the X-ray intensities for the (xn+p) and (xn+2p) cases is observed. This effect may be an indication for the influence of competing reaction channels, in particular due to the large break-up probability of the ^{6}Li nucleus, possible consequences of which are discussed in sect. 3.

Rel. X-efficiency ε_x^{rel}	< 5 %
σ_I (K-shell)	ca. 15 %
ω_K	< 1 %
X-ray intensity I_x	ca. 5 %
Target absorption B_x	< 3 %
Rel. γ-efficiency ε_γ^{rel}	ca. 5 %
Angular distribution of γ-rays	< 10 %
Conversion coefficient	ca. 5 %
γ-ray intensity I_γ	5-15 %

Tab. 4: Sources of experimental uncertainties of the measured compound nucleus cross sections

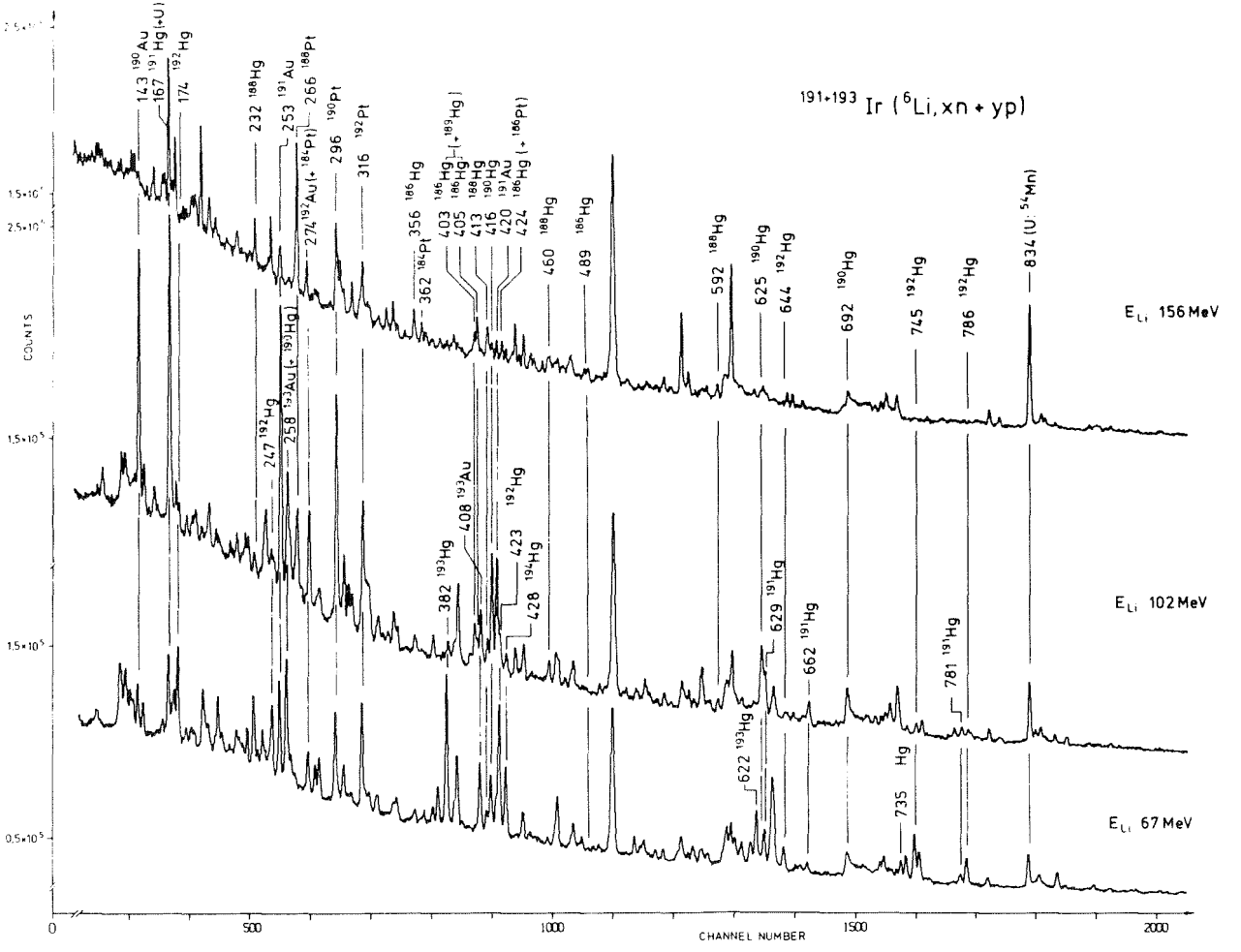

Fig. 4: γ-ray spectra of the $^{191+193}Ir(^{6}Li,(xn+yp)+\gamma)$ reaction taken at different projectile energies. Only two or three transitions of each nuclide identified are labelled. The intensity scales have been normalized in such a way that the intensity scale of the γ-peaks represent approximately the trends of the excitation functions

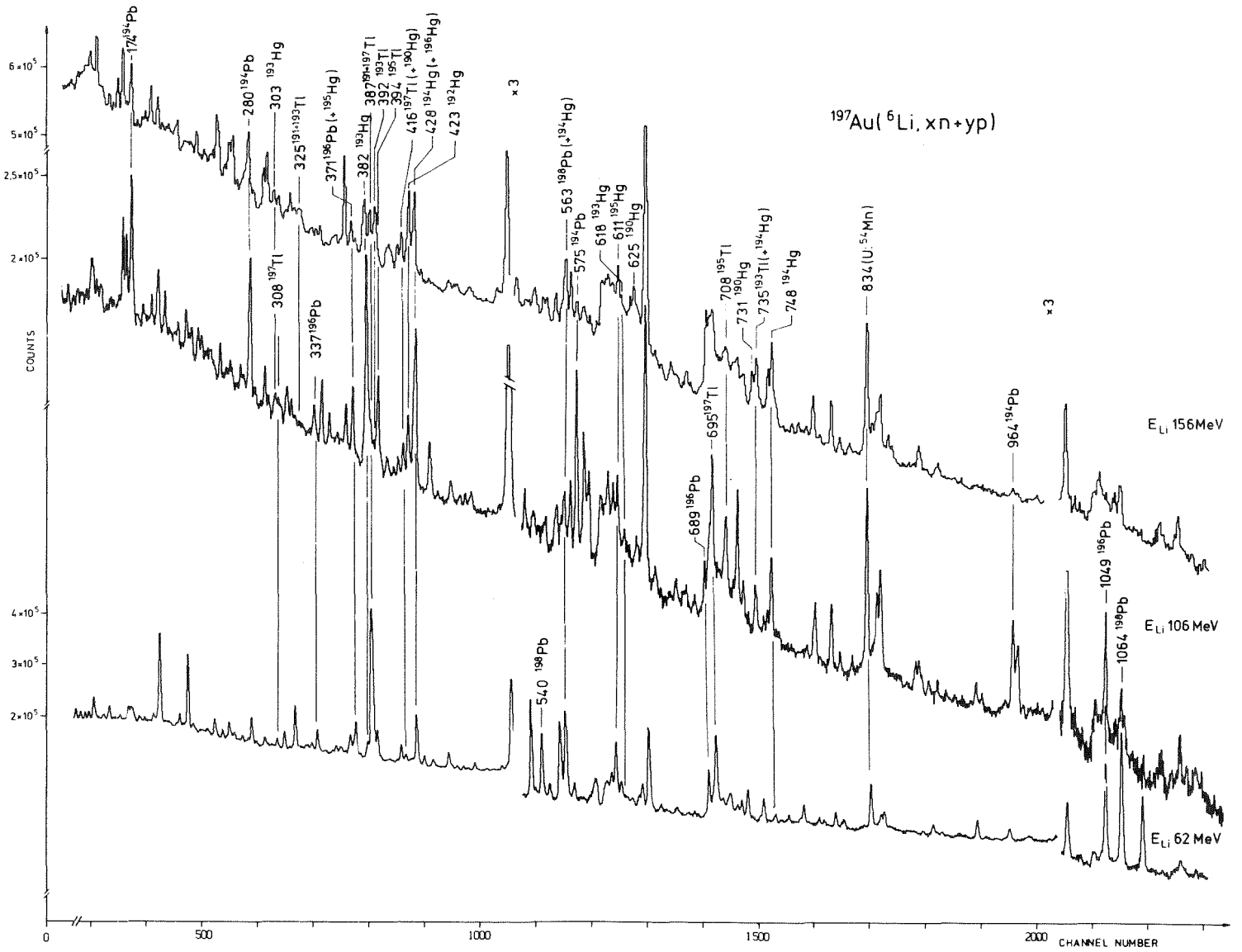

Fig. 5: γ-ray spectra of the $^{197}Au(^{6}Li,(xn+yp)+\gamma)$ reaction taken at different projectile energies. Only two or three transitions of each nuclide identified are labelled. The intensity scale have been normalized in such a way that the intensity scales of the γ-peaks represent approximately the trends of the excitation functions.

2.5 Competing Reactions

In the present experiments nuclear fission and the break-up of ^{6}Li are expected to be of some importance as reaction channels competing the compound reactions considered. Therefore some measurements were done in order to obtain at least estimates for the cross sections of these reactions.

2.5.1 Nuclear Fission

As a theoretical estimate of the fission cross sections seemed to be questionable due to our lack of knowledge of the values of the most important parameters (e.g. level density parameters a_f and a_n) we measured fission fragment spectra at E_{Li} = 146 and 113 MeV for the Au target using a 60 µm thick Si detector mounted perpendicular to the beam axis. Absolute fission cross sections have been derived by normalizing again to the simultaneously measured X-rays from the target and taking into account the angular distribution of fission fragments extracted from refs. [18),19)]. Tab. 5 presents results for the fission cross sections which prove to be small compared to the total reaction cross sections σ_R (calculated on the basis of the hybrid model - c.f. App. A).

The results are consistent with measurements of the $^{182}W(^{12}C,f)$ and $^{197}Au(\alpha,f)$ reactions [18),19)].

E_{Li} [MeV]	E_{CN} [MeV]	$\frac{d\sigma_f}{d\Omega}$ (90°) [mb/sr]	σ_f^{total} [mb]	σ_f^{tot}/σ_R
146	154	21.1	374	$14 \cdot 10^{-2}$
113	121	12.6	224	$9 \cdot 10^{-2}$

Tab. 5: Measured fission cross sections. The compound nucleus excitation energy E_{CN} includes the mass defect of the Au + ^{6}Li-system

2.5.2 ^{6}Li Break-up and Cluster Transfer

With increasing ^{6}Li energies a transition from pure Coulomb break-up to the break-up of ^{6}Li in the nuclear field is expected. In the course of separate experiments studying the break-up cross section at E_{Li} = 156 MeV we started to measure the spectra of the outgoing charged particles with a ΔE-E telescope for several targets. The telescope used consisted of a 200 µm thick Si surface barrier detector and a side entry Ge(Li) detector with an effective

sensitive depth of 32 mm mounted in an appropriate cryostat housing [20]. The ΔE-E signals have been measured in a two parameter list mode and sorted into particle specific spectra. Fig. 6 shows some of the particle spectra taken at a laboratory angle of 12^{o} with a ^{208}Pb target (8 mg/cm^2). The dominating role of a direct channel is obvious from the distinct broad bumps in the α-particle and deuteron spectra centered at about 2/3 and 1/3, of the incident ^{6}Li energy, respectively. Comparing the intensities of the α-particle and deuteron bumps there are conspicuously more α-particles than deuterons, an effect already observed in Coulomb break-up experiments [21] and suggesting some contribution of the three particle break-up. This may be indicated in the proton spectra. It should be noted here that up to now systematic studies of this type are actually hampered by the relatively low intensity of the 156 MeV ^{6}Li beam at the Karlsruhe cyclotron. A rough estimate from the α-particle bump results in a value of $d\sigma/d\Omega \sim 2.5$ b/sr for the differential cross section of reactions with at least an α-particle in the exit channel at $\theta_{Lab} = 12^{o}$ (^{208}Pb).

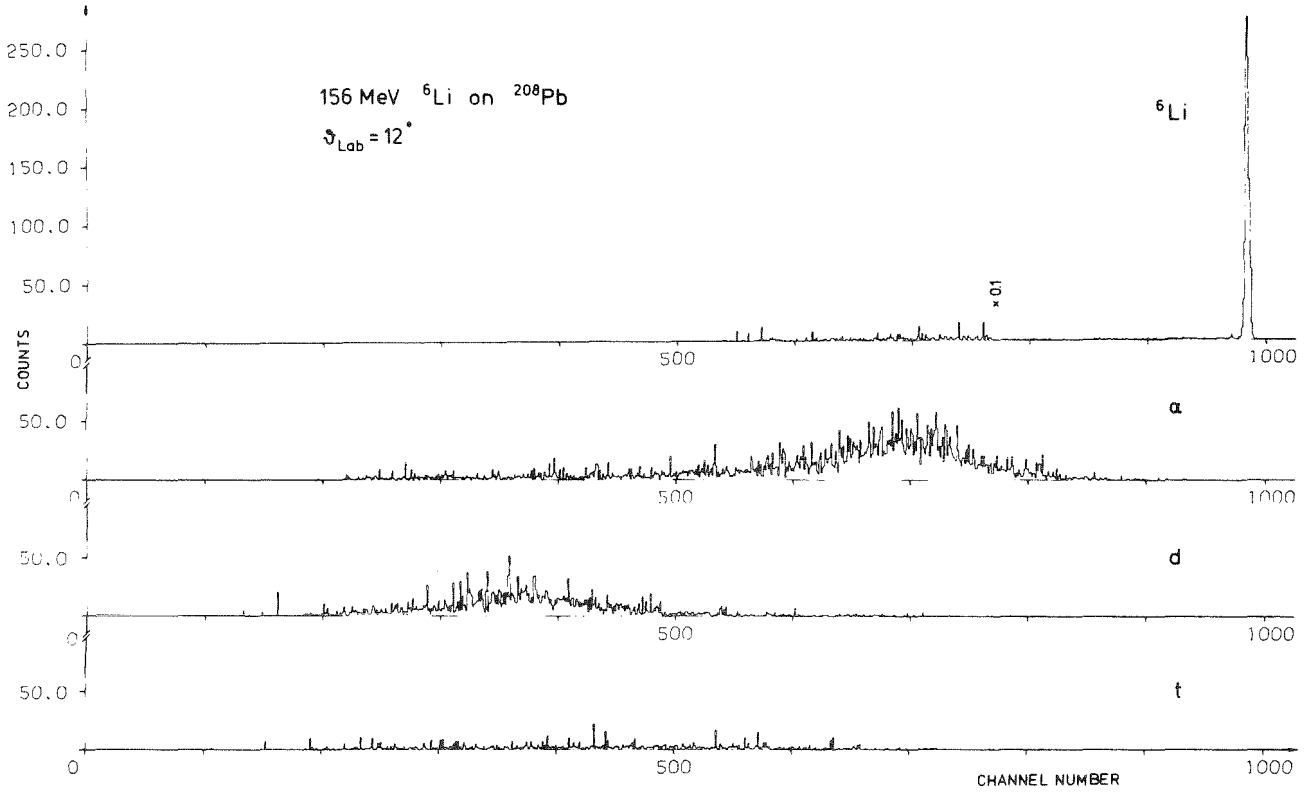

Fig. 6: Charged particle spectra of ^{6}Li induced reactions with ^{208}Pb measured with a ΔE-E telescope in a 130 cm Ø scattering chamber.

3. Excitation Functions

Fig. 7 presents an example of the experimental results for the excitation functions and gives an impression on the overall accuracy achieved. For a convenient comparison with theoretical predictions in the following we present smooth curves drawn through the experimental points as "experimental" excitation functions (fig. 8a-g). The relation between these "experimental" curves and the measured points is demonstrated in fig. 7.

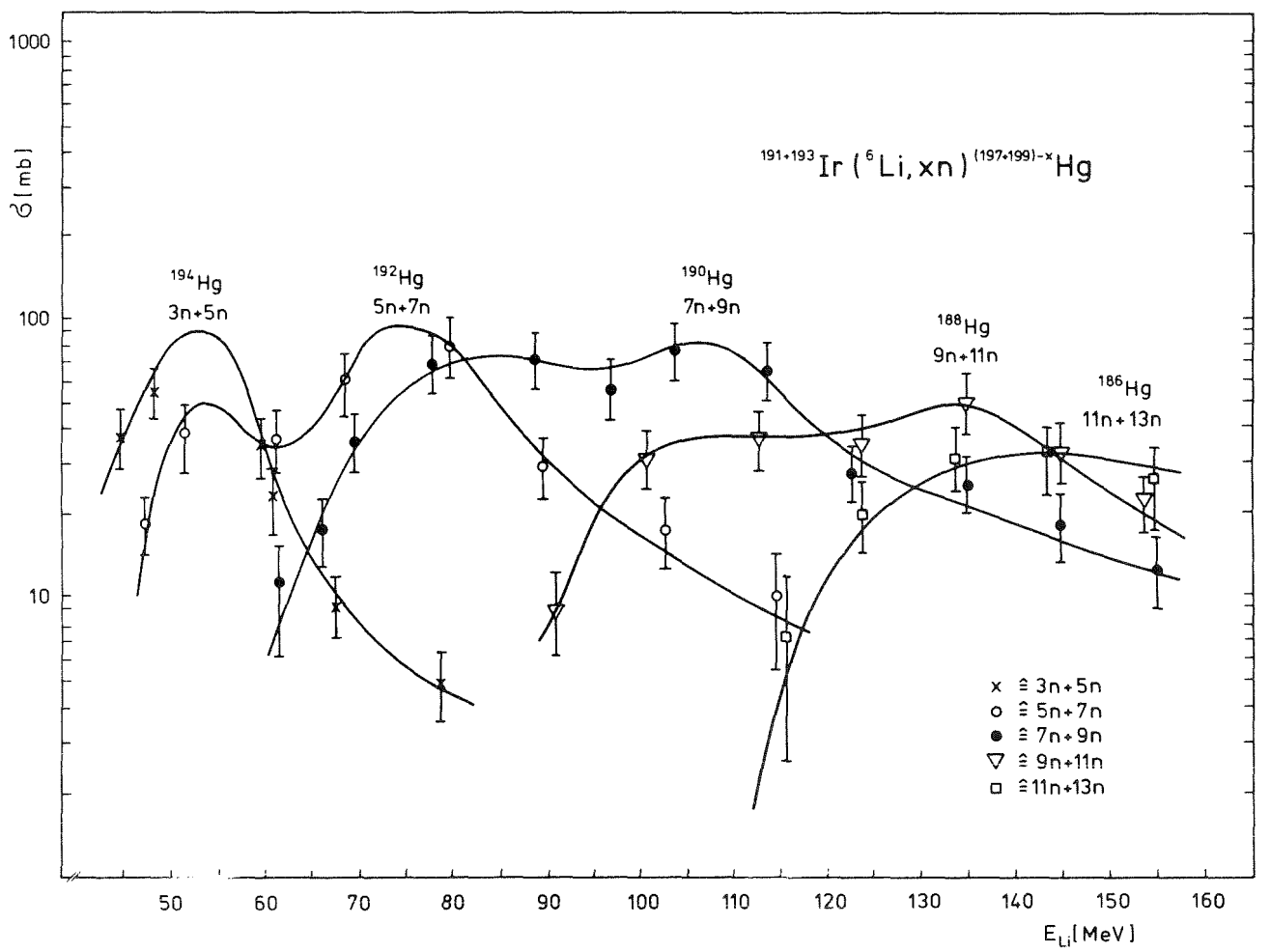

Fig. 7: Measured excitation functions $^{191+193}Ir(^{6}Li,xn)^{197+199-x}Hg$. The solid curves are drawn through the experimental points in order to guide the eyes

3.1 Hybrid Model Predictions

In Figs. 8a-g the experimental excitation functions are compared to results of calculations on the basis of Blann's hybrid preequilibrium model [8,9]. The idea and the main ingredients of this model, as well as the most important parameters and input data are briefly discussed in appendix A. In general, the calculations reproduce very well shapes and thresholds of the measured excitation functions, but the absolute scale of the theoretical curves have to be adjusted by reduction factors, the values of which are compiled in tab. 6. In the case of Ir (figs. 8a-e) two theoretical excitation functions have been added with normalizations corresponding to the isotopic ratio (^{191}Ir/^{193}Ir). In some cases discrepancies in the threshold position (e.g. for ^{197}Au(^{6}Li,8n+p) or in the shapes (^{197}Au(^{6}Li,6(8)n+2p)) are remarkable and cannot completely be ascribed to experimental uncertainties. The most conspicuous findings, however, are the considerable differences in the absolute values of experimental and theoretical cross sections and the anomalous relative enhancement of reactions with proton emission (see tab. 6).

Figs. 8a-g: Experimental (——) and (normalized) theoretical excitation functions

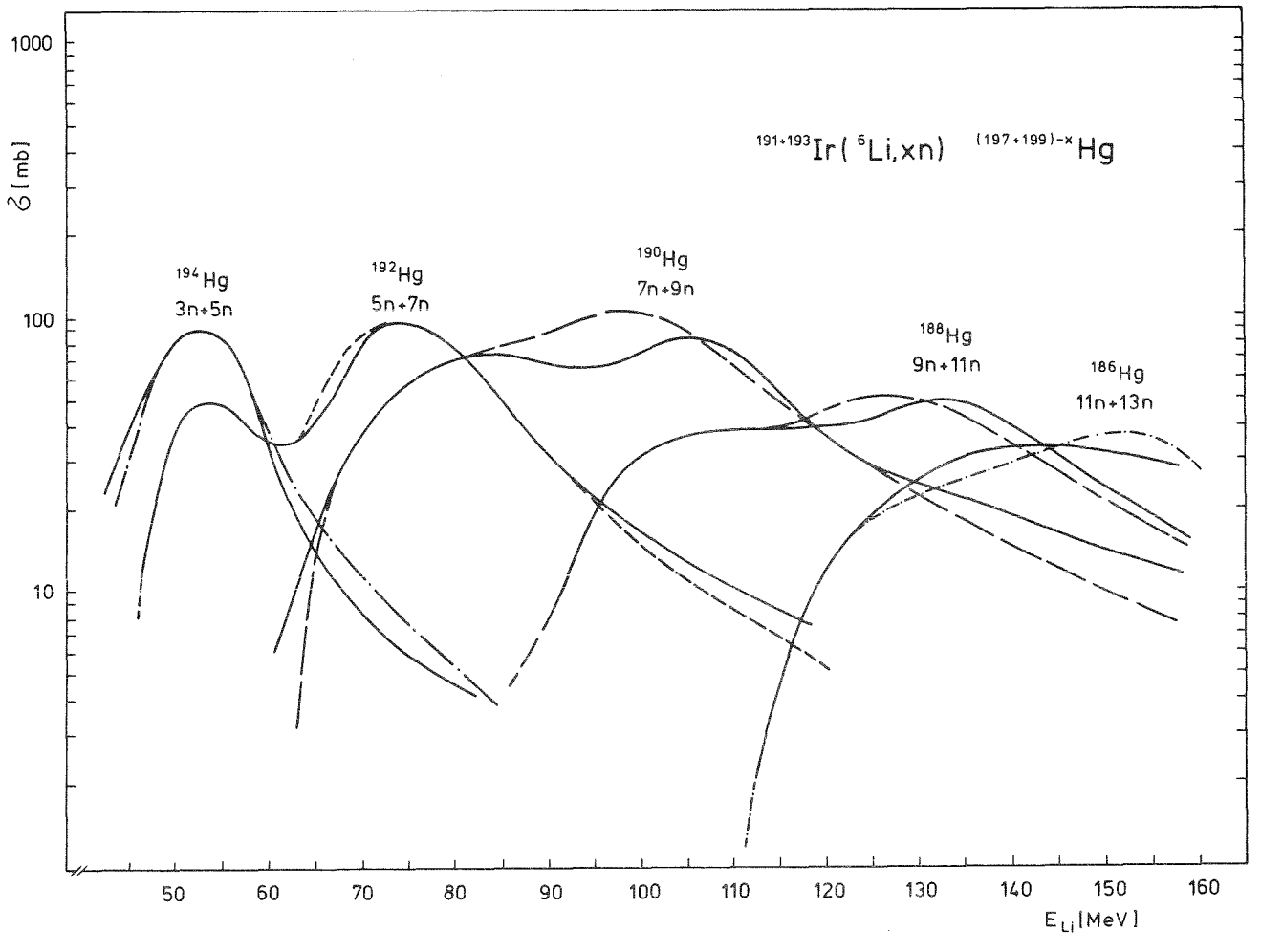

Fig. 8a

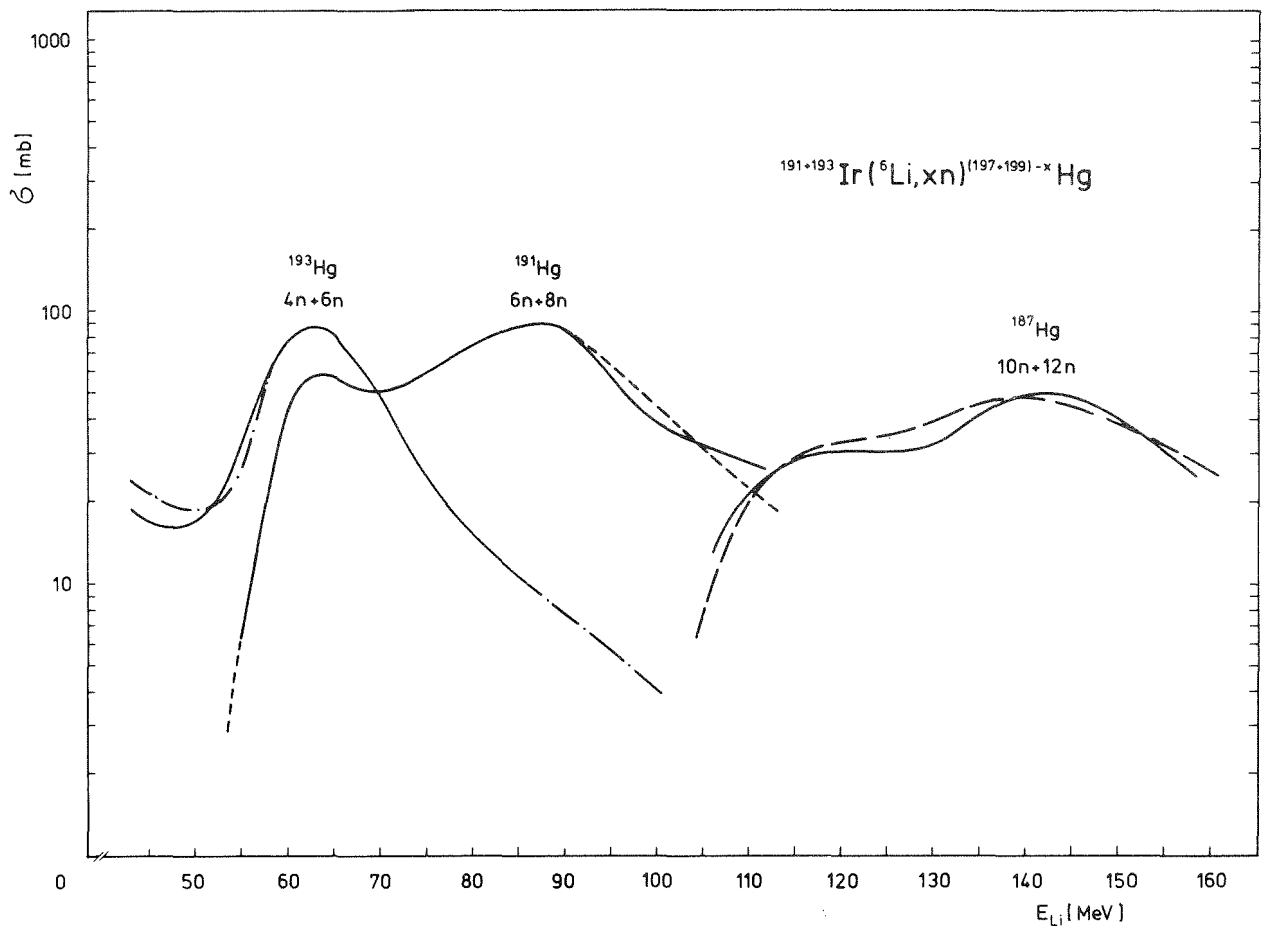
1000
100
10
0
σ [mb]
191+193Ir(6Li,xn)(197+199)-xHg
193Hg
4n+6n
191Hg
6n+8n
187Hg
10n+12n
50
60
70
80
90
100
110
120
130
140
150
160
ELi [MeV]

Fig. 8b

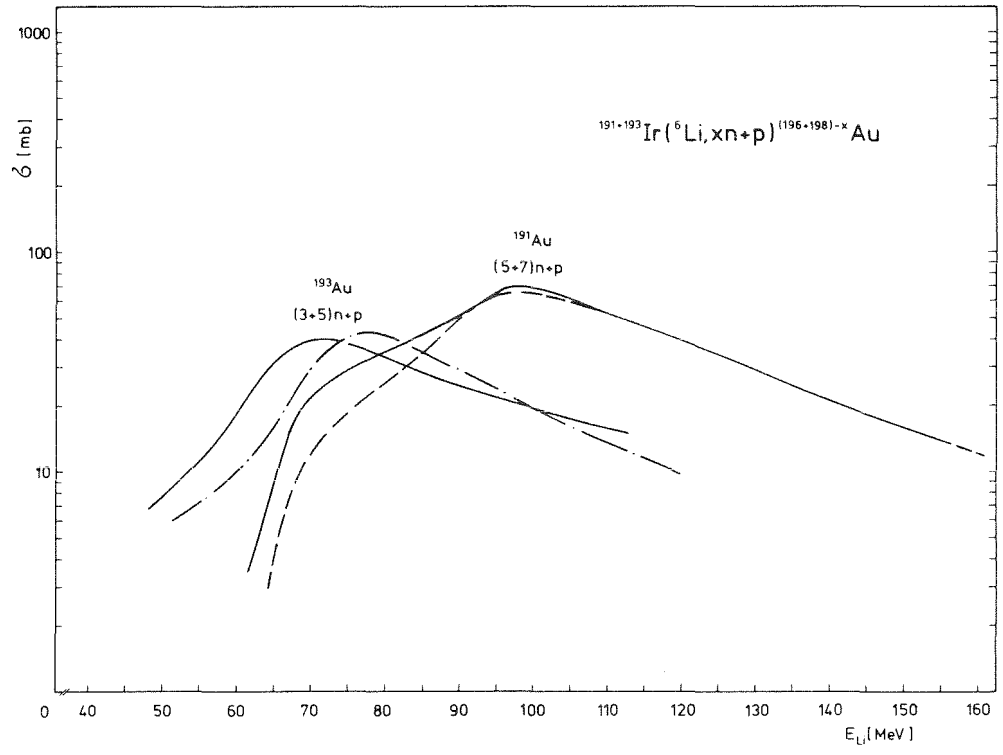
1000
100
10
0
σ [mb]
191+193Ir(6Li,xn+p)(196+198)-xAu
191Au
(5+7)n+p
193Au
(3+5)n+p
40
50
60
70
80
90
100
110
120
130
140
150
160
ELi [MeV]

Fig. 8c

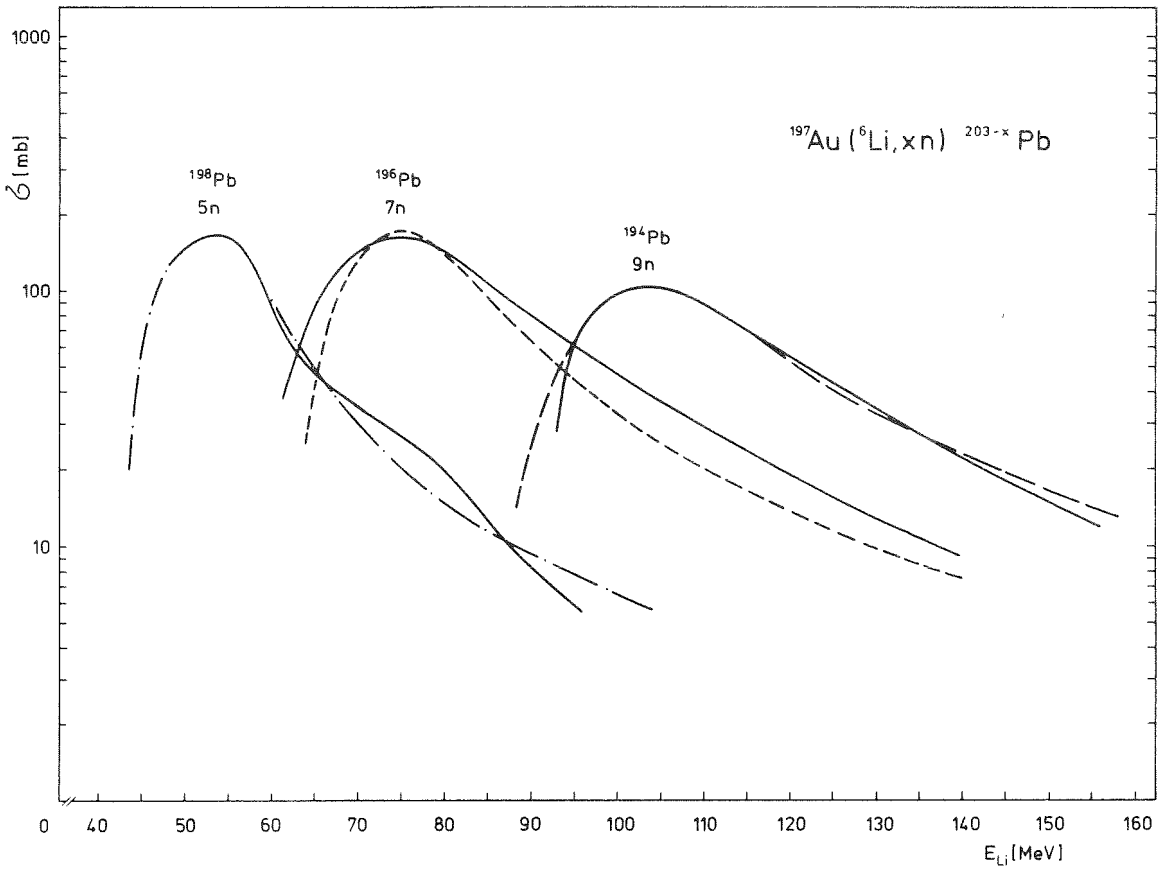
1000
100
10
σ [mb]
^{197}Au (^{6}Li, xn) $^{203-x}$Pb
^{198}Pb
5n
^{196}Pb
7n
^{194}Pb
9n
0
40
50
60
70
80
90
100
110
120
130
140
150
160
E_{Li} [MeV]

Fig. 8d

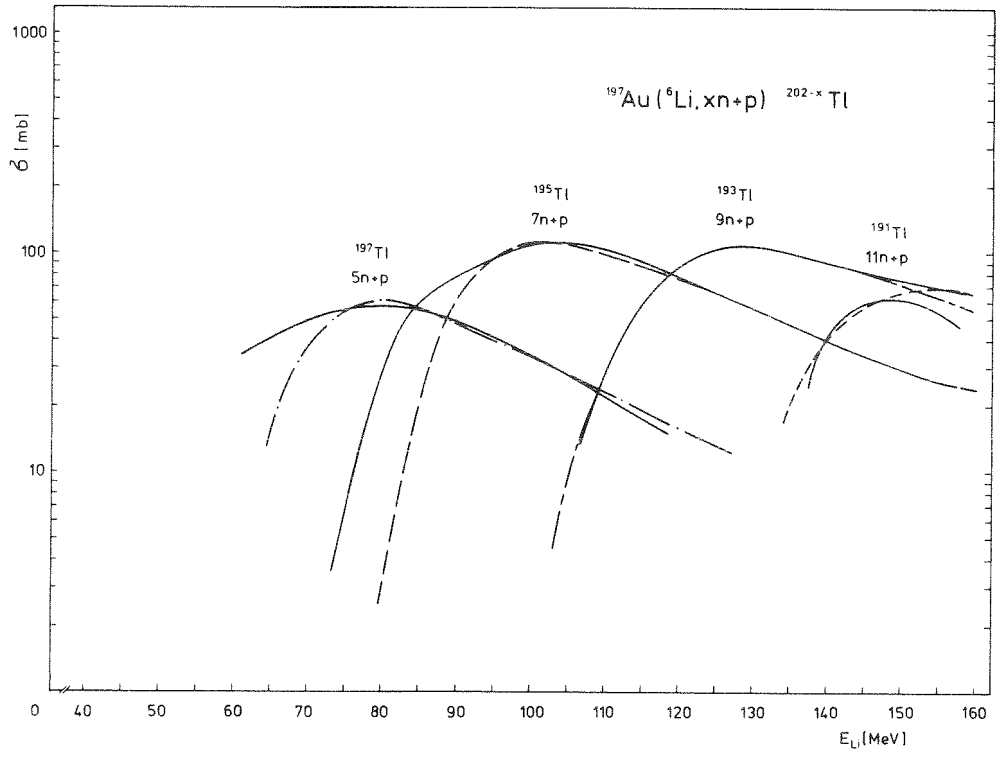
1000
100
10
σ [mb]
^{197}Au (^{6}Li, xn+p) $^{202-x}$Tl
^{197}Tl
5n+p
^{195}Tl
7n+p
^{193}Tl
9n+p
^{191}Tl
11n+p
0
40
50
60
70
80
90
100
110
120
130
140
150
160
E_{Li} [MeV]

Fig. 8e

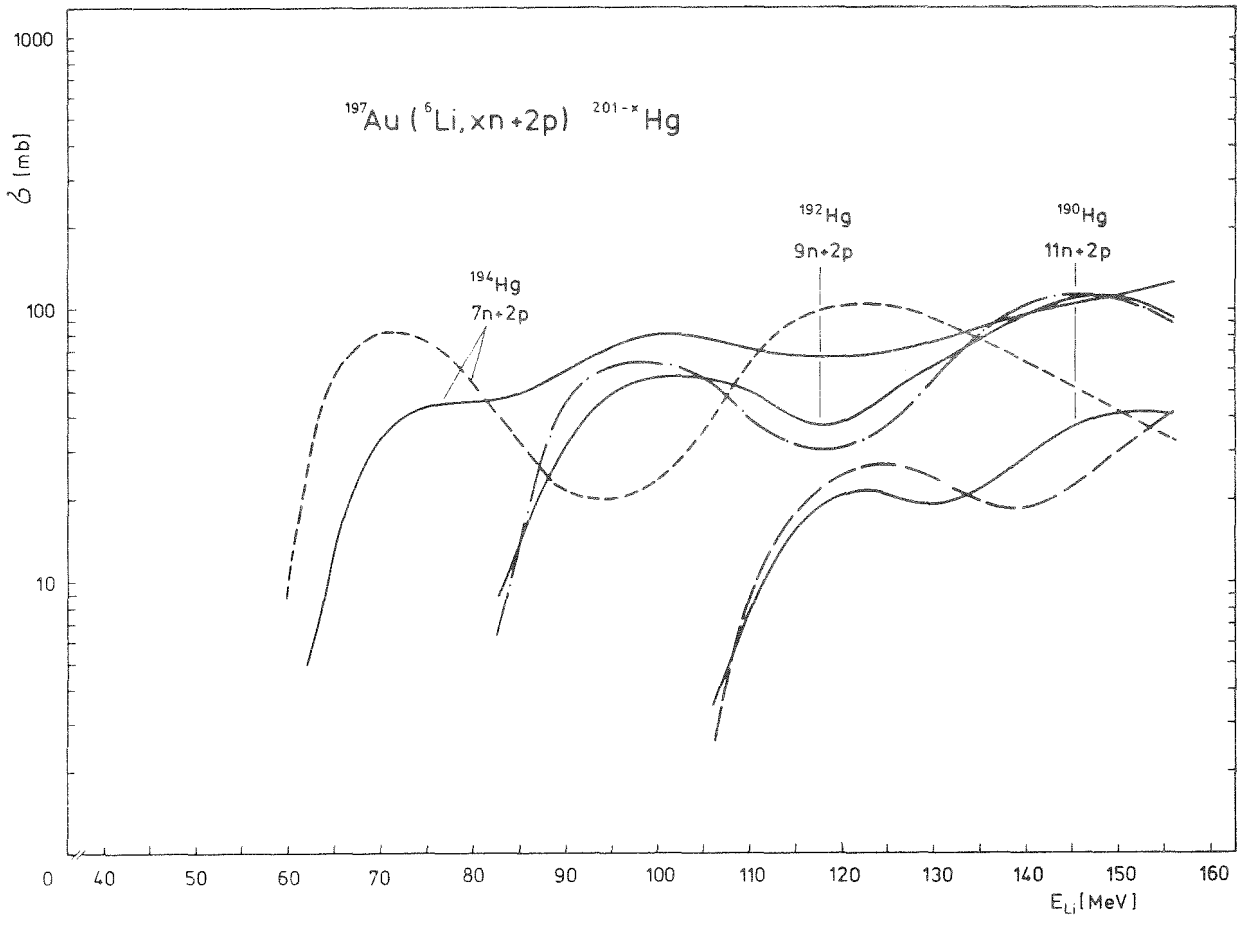
1000
100
10
0
σ [mb]
197Au (6Li, xn+2p) 201-xHg
194Hg
7n+2p
192Hg
9n+2p
190Hg
11n+2p
40
50
60
70
80
90
100
110
120
130
140
150
160
ELi [MeV]

Fig. 8f

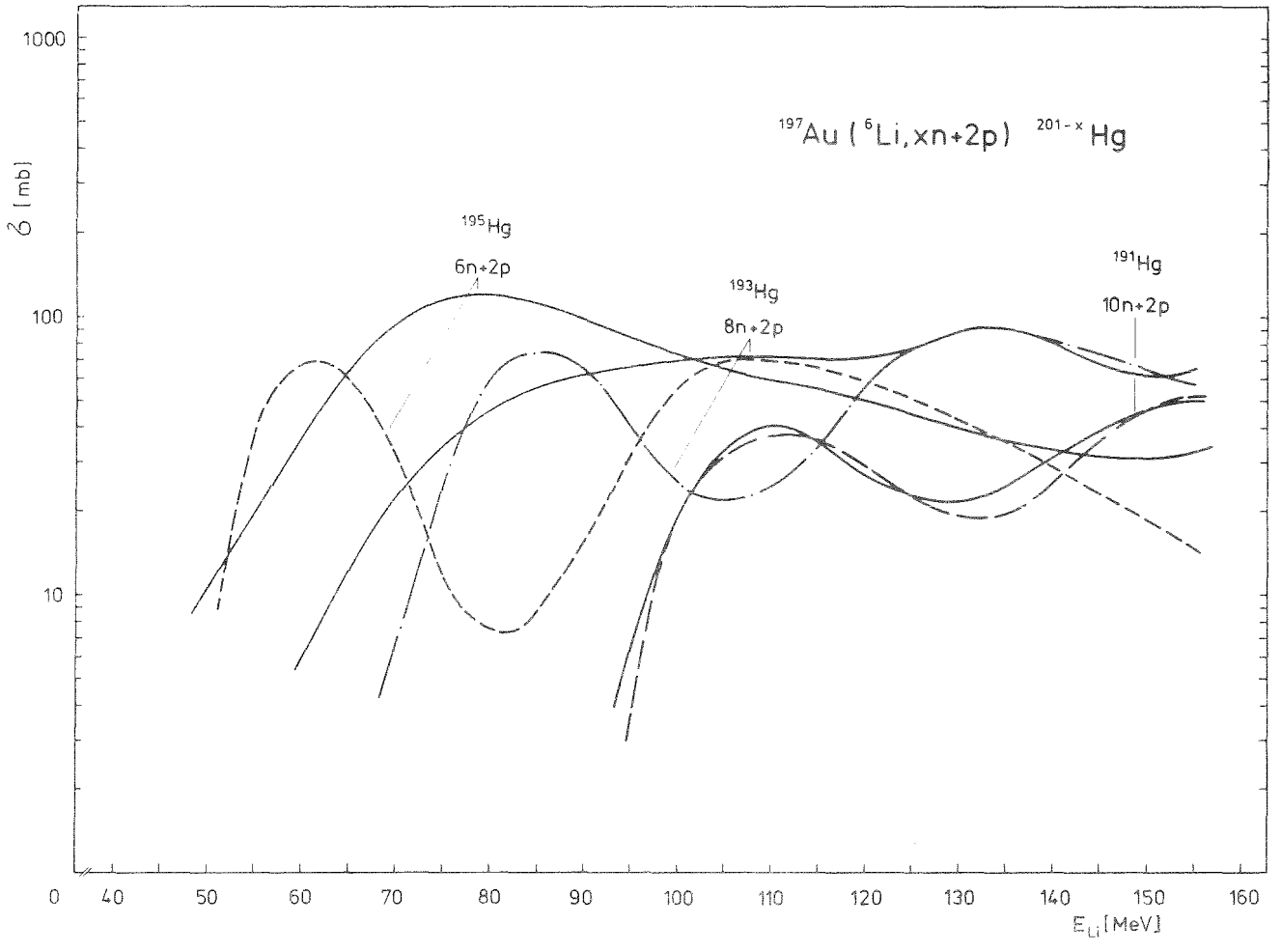
1000
100
10
0
σ [mb]
197Au (6Li, xn+2p) 201-xHg
195Hg
6n+2p
193Hg
8n+2p
191Hg
10n+2p
40
50
60
70
80
90
100
110
120
130
140
150
160
ELi [MeV]

Fig. 8g

Target										
^{197}Au	R	5n		7n		9n				
	F	6,5		6,5		6,5				
	R	5n+p		7n+p		9n+p		11n+p		
	F	2,2		2		2,8		3,5		
	R		6n+2p	7n+2p	8n+2p	9n+2p	10n+2p	11n+2p		
	F		0,15	0,3	0,4	0,9	1,8	3,7		
$^{191+193}Ir$	R	(3+5)n	(4+6)n	(5+7)n	(6+8)n	(7+9)n		(9+11)n	(10+12)n	(11+13)n
	F	6,5	7	6,9	6,8	5,1		6,9	6,8	7,7
	R	(3+5)n+p		(5+7)n+p						
	F	2		2,2						

Tab. 6: Reduction factors F for adjusting the calculated cross sections to the experimental curves in figs. 8a-g for all reactions R studied

3.2 Possible Effects Explaining the Anomalies and Discrepancies between Measured Cross Sections and Theoretical Results

We attempt to explain tentatively the observed discrepancies by possible shortcomings of the theoretical description. The fact that a satisfactory agreement has been found for $^{197}Au(\alpha,xn+yp)$ reactions up to E_α = 180 MeV [12] suggests that the discrepancies in the ^6Li case originate from particular features of ^6Li induced reactions. Besides the elastic scattering we have observed a dominating direct channel by break-up of the ^6Li-projectiles with or without transfer of one cluster into highly excited states which certainly reduces the probability for compound nucleus fusion. Therefore the usual approximations [9,13] in calculating transmission coefficients, reaction cross sections σ_R and compound nuclear cross sections σ_c may lead to overestimated values of σ_c. It should be noted that there are indications by deuteron induced compound nuclear reactions which may support the supposed role of the projectile break-up processes [11]. This more or less trivial effect implying a particular direct reaction cross section to be by far the largest contribution to σ_R can be checked more quantitatively as soon as realistic optical potentials for ^6Li scattering are available based on measurements in the energy range considered here.

In the excitation functions and the associated X-ray spectra we have observed an unexpected enhancement of (^6Li,xn+1 (2)p) reactions as compared to (^6Li,xn) reactions. This may be interpreted as a consequence of an "internal" break-up

of ^{6}Li. Well call "internal" break-up the effect that the ^{6}Li penetrating the nuclear field not completely looses the memory of its original structure and occupies with some preference cluster configurations in the beginning of the equilibration process from where one of the clusters is emitted by a direct stripping process (cluster transfer into highly excited states). With this view a (^{6}Li,xn+p) reaction e.g. may be regarded to contain a component of an (α,(x-1)n) compound nuclear reaction accompanied by emission of a spectator deuteron (or n-p pair). These reaction ways enhance the probability for (^{6}Li,xn+1(2)p) channels. Thus, though break-up is heavily preventing the complete fusion of ^{6}Li and of the target nucleus, one of the fragments is forming an ordinary compound nucleus. Independent from the interesting question to what extent such reactions quantitatively account to the observed anomalies, ^{6}Li reactions are most likely influenced by mechanisms of this mixed reaction type, which is certainly worthwhile to be investigated. In this context the experimental observation of different intensities in the deuteron and α-particle bumps of the spectra (c.f. sect. 2.3) may be of importance though this may mainly be due to (external) three particle break-up (^{6}Li $\rightarrow \alpha + p + n$).

4. Concluding Remarks

Though the hybrid model in the present form used proves to be a reasonable basis for describing ^{6}Li induced compound nuclear reactions experimentally investigated here, there are particular features possibly arising from the large break-up probability of the projectile which require a more detailed consideration of the processes of compound nucleus formation and of equilibration. The anomalies observed indicate the presence of an unusual mechanism: compound nuclear reaction of one cluster fragment accompanied by direct stripping of the other fragment ("internal" break-up). Certainly further experimental investigations are necessary to establish such a reaction type definitely, to clarify some open questions (influence on the shape of excitation functions) and to exclude alternative interpretations of the experiments. Some answers are expected from studies of the angular distribution, of the energy dependence and of α-d-coincidences of the ^{6}Li break-up process, from measurements of the proton spectra and of γ-rays coincident with break-up fragments.

We thank Prof. Dr. G. Schatz, Prof. Dr. L. Lassen and Dr. H. Schweickert for their interest, encouragement and valuable discussions. The experiments would have been impossible without the continuous support of the cyclotron crew and without the extreme efforts, in particular of Ing. F. Schulz, J. Biber and H. Kuhn in providing the ^{6}Li beam. We thank Prof. Dr. M. Blann for generously providing his computer code and for his advice.

References

1. Weisskopf, V.F., Ewing, D.H., Phys. Rev. 57 (1940) 472

2. Griffin, J.J., Phys. Rev. L. 17 (1966) 478

3. Harp, G.D., Miller, J.M., Berne, B.J., Phys. Rev. 165 (1968) 1166

4. Blann, M., Phys. Rev. L. 21 (1968) 1357

5. Harp, G.D., Miller, J.M., Phys. Rev. C3 (1971) 1847

6. Cline, C.K., Blann, M., Nucl. Phys. A172 (1971) 225

7. Blann, M., Phys. Rev. L. 27 (1971) 337

8. Blann, M., Phys. Rev. L. 28 (1972) 757

9. Blann, M., Lect. Notes, Int. School on Nucl. Phys., Predeal, Romania, Sept. 1974

10. Haushahn, G., Möllenbeck, J., Schatz, G., Schulz, F., Schweickert, H., Proc. 7. Int. Conf. on Cyclotrons and their Applications (Birkenhäuser, Basel, 1975) p. 376

11. Jahn, P., Probst, H.-J., Djaloeis, A., Davidson, W.F., Mayer-Böricke, C., Nucl. Phys. A209 (1973) 333

12. Jahn, P., Probst, H.-J., Djaloeis, A., Davidson, W.F., Mayer-Böricke, C., Nucl. Phys. A250 (1975) 149

13. Thomas, T.D., Phys. Rev. 116 (1959) 703

14. Habs, D., Klewe-Nebenius, H., Löhken, R., Göring, S., van Klinken, J., Rebel, H., Schatz, G., Z. Physik 250 (1972) 179

15. Bambynek, W., Crasemann, B., Fink, R.W., Freund, H.-V., Mark, H., Swift, C.Q., Price, R.E., Venugopala, R.D., Rev. Mod. Phys. 44 (1972) 716

16. Garcia, J.D., Fortner, R.J., Kavanagh, T.H., Rev. Mod. Phys. 45 (1973) 111

17. Kropp, J., Diploma Thesis, University of Heidelberg (1976) unpublished

18. Gindler, J., Münzel, H., Buschmann, J., Christaller, G., Michel, F., Rohde, G., Nucl. Phys. A145 (1970) 337

19. Sikkeland, T., Phys. Rev. 135 (1964) B669 ; Sikkeland, T., Clarkson, J.E., Naftali, H., Steiger, S., Viola, V.E., Phys. Rev. C3 (1971) 329

20. Gils, H. J., Rebel, H., Hartmann, D., Riepe, G., Protic, D., KFK Report No. 2233 (1975) contrib. 6.18

21. Pfeiffer, K.O., Speth, E., Bethge, K., Nucl. Phys. A206 (1973) 545

22. Blann, M., Private communication

23. Myers, W.D., Swiatecki, W.J., Nucl. Phys. 81 (1966) 1 and Proc. Int. Symp. on Nuclides far off the Stability, Lysekil, Sweden (1966)

24. Garvey, G.T., Gerace, W.J., Jaffe, R.L., Talmi, J., Kelson, J., Rev. Mod. Phys. 41 (1969) S1

25. Münzel, H., Buschmann, J., Christaller, G., Hartmann, D., Hartwig, D., Michel, F., Schneider, R., Schwarzbach, E., Nucl. Inst. Meth. 73 (1969) 103

Appendix A: Hybrid Model Calculations

Several reaction models [2-9] have been worked out describing the high energetic tails of experimentally observed excitation functions by the emission of high energetic particles from the compound nucleus before the thermal equilibrium has been reached. In the hybrid model of Blann et al. [8,9] the state just after fusion of projectile and target nucleus is characterized by the target nucleons occupying the levels below the fermi edge and the projectile nucleons being in levels high above the fermi edge. The reaction is assumed to proceed through a series of two-body scattering processes with either rescattering or particle emission into the continuum and leading to states with increasing numbers of particles above and holes below the fermi level up to an equilibrium value $\bar{n}$. The actual number of particles and holes - the exciton number n - classifies the actual state. It is generally assumed that the equilibration process proceeds by particle-hole pair creation, that means, n progresses from an initial value n_o by increments of 2 to the equilibrium value $\bar{n}$. The simplest description of the preequilibrium decay rests in the statistical assumption that every particle-hole configuration for a given exciton number occurs with equal a-priori probability, controlled by the density of the accessible levels for the energy actually available and limited by the Pauli principle. For each of these exciton states the probability for one particle to be emitted into the continuum is calculated.

The essential quantities involved in the basic concept may be seen from the general formula [9] describing the preequilibrium particle energy spectrum

$$\left(\frac{d\sigma}{d\varepsilon}\right)_x = \sigma_c \sum_{n=n_o}^{\bar{n}} p_n^x \left[\frac{\rho_n(U,\varepsilon)}{\rho_n(E)}\right] \left[\frac{\lambda_c(E)}{\lambda_c(\varepsilon) + \lambda_{n+2}(\varepsilon)}\right] \cdot D_n \qquad (A.1)$$

Here x denotes the type of the emitted particle, p_n^x the number of particles x in the n-exciton configuration, $\rho_n(E)$ the number of configurations for which n excitons share a total energy E, $\rho_n(U,\varepsilon)$ the number of combinations having n excitions such that one particle could be emitted[+] with the energy between ε and $\varepsilon + d\varepsilon$ leaving the remaining excitons sharing the residual excitation energy $U = E - \varepsilon - B_x$ (B_x = particle binding energy). The expression in the first set of brackets is just the number of nucleons of type x in the energy intervall ε to $\varepsilon + d\varepsilon$ of a n-exciton state. The quantities in the second set of brackets represent the fraction of particles emitted into the continuum ($\lambda_c(\varepsilon)$ = decay rate into the continuum, λ_{n+2} = intranuclear transition rate

[+] Actually only the emission of one particle into the continuum is considered.

to the n+2 exciton state). The depletion factor D_n reduces the population of each state according to the amount of particle emission from simpler states.

For an evaluation the quantities in (A.1) must be specified adequately or substituted by other ones which are more easily accessible. The procedures doing so imply certain approximations and simplifications. The present calculations have used the computer code ALICE (including the precompound routine HYBRID) by M. Blann [22] which provides, among others, routines for calculating the following necessary quantities:

(i) The cross section σ_c for compound nucleus formation by use of the approximation of Thomas [13], which has proven to be questionable in our case due to the large contribution of ^{6}Li break-up to the reaction cross section. With certain restrictions the code includes the possibility to take into account the fission process. Since the measured cross sections σ_f were very small we did not use this option.

(ii) The level densities according to formulas discussed in the original papers (see ref. 7,9).

(iii) The nucleon binding energies B_x according to the mass formula of Myers and Swiatecki [23]. The alternative use of Garvey's values [24] had minor influence on the calculated excitation functions.

(iv) In contrast to earlier exciton models the hybrid model calculates absolute spectral yields as the intranuclear transition rates $\lambda_{n+2}(\epsilon)$ are evaluated through use of the nucleon-nucleon scattering cross sections. The calculation of the decay rate into the continuum λ_c needs the values of the cross sections for the inverse reactions.

In addition to the parameters specifying the specific reaction under consideration the initial exciton number n_o is an input parameter the importance of which is not quite clear. In the hybrid model n_o is the sum of protons and neutrons above and of holes below the fermi level in the intial state. The present calculations used sets of n_o = 3p + 3n + 1h = 7 for Ir(^{6}Li,xn) and Ir(^{6}Li,xn+p) reactions, n_o = 3p + 3n + 0h = 6 for ^{197}Au(^{6}Li,xn) and ^{197}Au(^{6}Li,xn+p) reactions, and n_o = 4p + 3n + 0h = 7 for ^{197}Au(^{6}Li,xn+2p) reactions.